

## Stick-slip behavior of a clayey crustal fault

Jun Kameda<sup>1,\*</sup> and Yohei Hamada<sup>2</sup><sup>1</sup>*Department of Earth and Planetary Sciences, Graduate School of Science, Hokkaido University, N10 W8, Sapporo 060-0810, Japan*<sup>2</sup>*Kochi Institute for Core Sample Research, Japan Agency for Marine-Earth Science and Technology, Nankoku 783-8502, Japan*

(Received 14 May 2021; accepted 6 February 2022; published 18 March 2022)

Recent studies have revealed that slip on clay-rich fault planes, which develop in the shallow crust and can cause huge earthquakes, is controlled by their flow properties rather than their frictional properties. Here, we simulate a seismogenic crustal fault and show that such a fault plane may behave as a thixotropic yield stress fluid. We then conduct numerical experiments using a simple spring-slider model that incorporates this thixotropic property, and we successfully reproduce spontaneous stick-slip behaviors that correspond to a variety of seismogenic processes, ranging from regular earthquakes with high slip rates to slow earthquakes with lower slip rates. This finding suggests that the seismic activity on a shallow clay-rich crustal fault may be governed by the time-evolving microstructure of the clay-water system that exists along the fault plane.

DOI: [10.1103/PhysRevResearch.4.013211](https://doi.org/10.1103/PhysRevResearch.4.013211)

## I. INTRODUCTION

Earthquakes are caused by the rupture and slip of faults in Earth's crust. It is generally thought that the slip behavior of a fault is governed by the frictional resistance acting on the solid contact surfaces of the constituent materials (i.e., rocks and minerals) [1]. However, it has been shown that faults in the shallow crust, which are characterized by a layer of clay minerals on the fault plane, may behave like a viscoplastic fluid. An archetypal example is the March 2011 Mw 9.0 Tohoku-Oki megathrust earthquake that occurred on a plate-boundary fault off the coast of Tohoku, Japan [2]. The shallow part of this fault, which is generally considered nonseismogenic, experienced large ( $\sim 50$  m) and fast ( $\sim 1$  m s<sup>-1</sup>) coseismic displacement and generated a huge tsunami [2–4]. It has also been shown that precursory seismic activities with slower slip velocities occurred before the mainshock on this fault [5–7]. A drilling survey was conducted 1 y after the earthquake to investigate the material and mechanical properties of the fault, revealing that the fault zone is composed of 60–80 wt. % smectite [8,9]. Rheological experiments that simulated a fault zone (i.e., a mixture of smectite and quartz dispersed in saline water) have demonstrated that the shear force of the fault could be controlled primarily by the cohesion of clay minerals and that a plate-boundary fault could behave as a viscous fluid during an earthquake [10,11]. However, it is unclear how fault slips with various slip velocities that range from regular to slow earthquakes coexist on the same fault plane and how each slip event interacts physically with

other slip events, thereby highlighting the need for further research on the rheological behavior of the fault. It is therefore essential to examine whether such a clay-rich fault with a fluidlike property can exhibit spontaneous stick-slip behavior. In general, clay suspensions often exhibit yield stress fluid behavior [12,13], such that they begin to flow abruptly and accelerate when subjected to stress above a critical threshold. This property of clay and soil suspensions has been invoked to explain avalanche dynamics [12,14,15]. Coussot *et al.* [12,13] have developed a simple model to describe the behavior of such a yield stress fluid by introducing the state variable of suspension structure  $\lambda$ , which likely evolves as a result of competition between aging and rejuvenation:  $\frac{d\lambda}{dt} = \frac{1}{\tau} - \alpha\lambda\dot{\gamma}$ , where  $\alpha$  is a system-dependent constant,  $\tau$  is the characteristic time of the buildup of the microstructure at rest,  $\dot{\gamma}$  is the shear rate, and  $t$  is the time. The state variable  $\lambda$  is then related to the flow properties (specifically, the suspension viscosity  $\eta$ ) by  $\eta = \eta_0(1 + \lambda^n)$ , where  $\eta_0$  is the limiting viscosity at high shear rates. As the fault zone system of the Tohoku plate-boundary fault can be approximated by a clay suspension, we expect that fault movement will accordingly exhibit a yield stress fluid behavior and that this behavior will govern earthquake generation. The fact that the yield stress fluid can cause stick-slip motion has been observed by the rheological experiments of Pignon *et al.* [16]. A rheological model like that of Coussot *et al.* [12,13] has been studied by Picard and Ajdari [17], who demonstrated numerically that oscillations between frozen and flowing states can occur at imposed shear rates. Here, we first investigate the possibility of the thixotropic behavior of a clay-water system along a crustal fault via rheological experiments. We then conduct numerical experiments to examine the possibility that such a system exhibits stick-slip behavior that could correspond to cyclic seismic activity. We finally discuss the relationship between the behavior observed in this paper and the natural seismic activity observed on shallow clay-rich plate-boundary faults.

\*kameda@sci.hokudai.ac.jp

Published by the American Physical Society under the terms of the [Creative Commons Attribution 4.0 International license](https://creativecommons.org/licenses/by/4.0/). Further distribution of this work must maintain attribution to the author(s) and the published article's title, journal citation, and DOI.

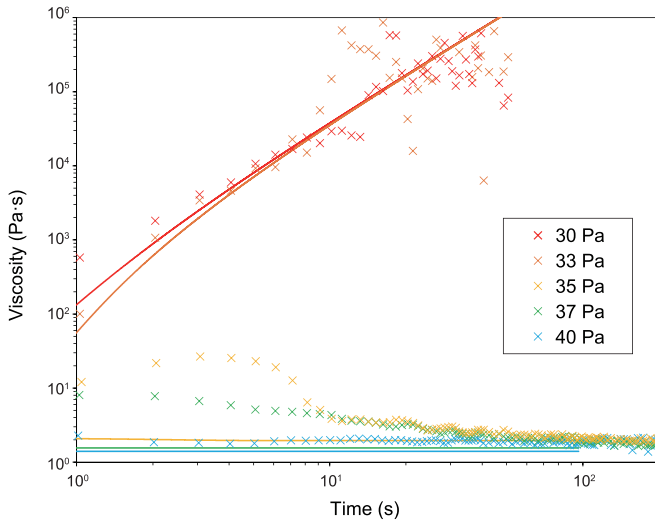


FIG. 1. Rheological behavior of a clay suspension (70 wt. % smectite + 30 wt. % quartz) in brine (solid fraction = 0.12), with viscosity bifurcation at a critical stress of 34 Pa illustrated. Each solid line (of the same color) was drawn by integrating the equation in Coussot *et al.* [12,13] with a set of fitting parameters ( $\alpha = 1.03$ ,  $\tau = 0.059$  s,  $\eta_0 = 1.06$  Pa·s, and  $n = 2.06$ ) under the respective stress conditions.

## II. RHEOLOGICAL EXPERIMENTS

The samples in our experiments were prepared by mixing smectite (70 wt. %) and quartz (30 wt. %) powders dispersed in a 0.6 M NaCl solution at a solid fraction of  $\sim 0.12$ . Rheological tests were conducted using a stress-controlled rheometer (HR-2, TA Instruments) at 25 °C and a constant stress. The details of the experimental system can be found in Kameda and Hamada [11]. The major difference from the experimental setup of Kameda and Hamada [11] is that we did not preshear the sample to avoid disturbing the suspension structure.

Figure 1 shows the results of the rheological tests under various stress conditions. The viscosity of the sample bifurcated at a critical applied stress of 34 Pa. Above this stress level, the viscosity decreased gradually with increasing strain and eventually converged to approximately the same value ( $\sim 2$  Pa·s), while the viscosity increased progressively to  $> 10^5$  Pa·s (the strain rate was below the detection limit at this time) when the applied stress was below the critical value. We note that the critical stress of 34 Pa is generally consistent with the yield stress from the standard flow curve of the sample [32.4 Pa; 11]. The observed viscosity bifurcation is also in agreement with previous tests that employed a comparable system and thixotropic yield stress fluids [12,13].

We performed an inversion analysis of the present data using the model of Coussot *et al.* [12,13] with a least-squares fitting approach. This model explained the observed experimental behavior using the following set of fitting parameters:  $\alpha = 1.03$ ,  $\tau = 0.059$  (s),  $\eta_0 = 1.06$  (Pa·s), and  $n = 2.06$  (Fig. 1). Coussot *et al.* [12,13] assigned a value of  $n = 2.0$  for a bentonite suspension with a solid fraction of 0.04; we obtained a comparable  $n$  value for the present system with a much higher solid fraction in brine, which suggests that  $n$  is not particularly sensitive to either the solid fraction or

chemical condition. However, the *in situ* solid fraction of the Tohoku plate-boundary fault zone is  $\sim 0.6$  [10] and is even higher at greater depth; accordingly, the remaining variables require appropriate adjustments when considering the behavior of the natural fault. Next, we tentatively considered the possible faulting process by employing the expected parameter values for the *in situ* conditions of the plate-boundary fault.

## III. EARTHQUAKE CYCLE SIMULATIONS USING A SPRING-SLIDER MODEL

We considered a simple spring-slider model to examine the dynamics of the plate-boundary fault. The model for earthquake cycle simulations is typically constructed by connecting in series a spring and a slider that obeys a time-evolving friction law [1]. However, based on the above experimental results, the slider in this model was assumed to be regulated by the rheology of the yield stress fluid:  $m \frac{d^2x}{dt^2} = k_0(V_{pl}t - x) - \sigma$ , where  $k_0$  is the spring constant, and  $V_{pl}$  is the loading velocity of the plate. The shear stress  $\sigma$  of the fault is described by  $\sigma = \eta \dot{\gamma} = \frac{\eta_0}{w} (1 + \lambda^n) \frac{dx}{dt}$ , where  $w$  is the thickness of the slip plane. The following values were adopted for this paper:  $k_0 = 5.0 \times 10^6$  Pa m $^{-1}$ ,  $V_{pl} = 8.0$  cm y $^{-1}$ , and  $m = 2.0 \times 10^6$  kg m $^{-2}$ , which correspond to a depth of  $\sim 1$  km below the sea floor [8], and  $w = 1$  cm [11]. We varied  $\alpha$  over the 0.1–10 range. The limiting viscosity  $\eta_0$  was assumed to be  $10^5$  Pa·s (which is five orders of magnitude greater than the experimental value) and was calculated using the expected scaling between the experimental and natural fault zones [11]. The above equation was solved numerically using either a fifth-order Runge-Kutta method or a solver for differential equations in MATLAB.

Figure 2(a) shows the temporal changes in the slip velocity, shear stress, viscosity, and state variable in a simulation with  $\alpha = 1.0$  and at  $\tau = 2400$  s. The periodic oscillations in the shear stress signal are characteristic of spontaneous stick-slip motion within the system. If  $\tau$  is reduced, then the recurrence interval of stick-slip events increases ( $\sim 30$  y at  $\tau = 1600$  s), and both the slip distance of the events and slip velocity increase [ $\sim 2.5$  m and  $\sim 0.9$  m s $^{-1}$ , respectively; Fig. 2(b)]. These observations can be explained qualitatively as follows. Rapid aging (i.e., smaller  $\tau$ ) causes the slider to stick, thereby facilitating a buildup of elastic energy in the spring that is eventually released by rapid earthquake slip. Conversely, slow aging does not allow the sufficient storage of elastic energy; in fact, a longer  $\tau$  yields smaller recurrence intervals with reduced slip distances for the events and lower slip velocities [Fig. 2(c)], and the system eventually transitions to a stable slip regime (i.e., without stick-slip motion). In this stable slip regime, the system reaches a steady state (i.e.,  $\lambda = 1/\alpha\tau\dot{\gamma}$ ), and the stress follows the relation  $\sigma = \eta \dot{\gamma} = \eta_0 \dot{\gamma} [1 + (\alpha\tau\dot{\gamma})^{-n}]$ , where  $\dot{\gamma} = 2.5 \times 10^{-7}$  (equivalent to the rate of plate motion divided by the fault zone thickness) at steady state, which leads to  $\sigma = \sim 44$  kPa at  $\tau = 3000$  s. We note that, although these adopted variables might have large uncertainties, they might be realistic, as  $\tau$  values on the order of several thousand seconds are close to the equilibration time of clay packing around the fault rocks predicted from swelling experiments [10]. Furthermore, the amplitude of the modeled

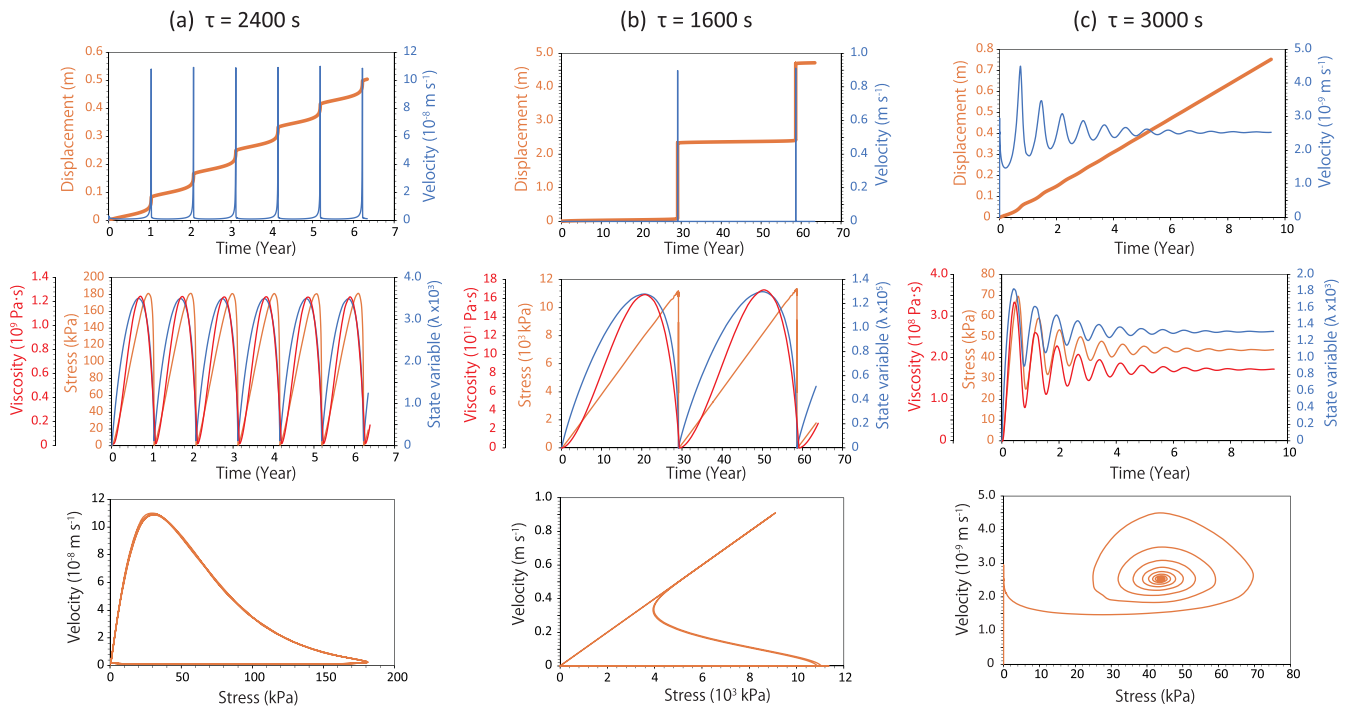


FIG. 2. Time histories of cumulative fault displacement and slip velocity (upper panels) and shear stress and state variable (middle panels) for (a)  $\tau = 1600$  s, (b)  $\tau = 2400$  s, and (c)  $\tau = 3000$  s ( $\alpha = 1$ ,  $\eta_0 = 1.0 \times 10^5$  Pa·s, and  $n = 2.0$ ). The lower panels show the velocity-stress relationships.

shear stress fluctuations [Fig. 2(a)] within the stick-slip regime is in the range of several hundreds of kilopascals, which is in agreement with the coseismic shear stress of the fault deduced from borehole observations [18]. The peak velocities of stick-slips were also reproduced in a variety of ways and spanned the regular earthquake ( $1 \text{ m s}^{-1}$ ) to slow-slip ( $\sim 10^{-7} \text{ m s}^{-1}$ ) range [5–7]. The above parameters should be better quantified through future experiments that employ the appropriate apparatus under fault-relevant conditions; here, we will further examine the validity of these simulations through numerical experiments. Figure 3 shows the relationship between the recurrence interval of stick-slip for different  $\alpha$  values (0.1, 1, and 10), and stress drop [Fig. 3(a)] and peak velocity [Fig. 3(b)]. The recurrence interval of stick-slip and the magnitude of the stress drop generally decrease with increasing  $\alpha$  [Fig. 3(a)]. The stress drop during each stick-slip event, which likely corresponds to slow slip, is  $\sim 1$ , 0.1, and 0.01 MPa when  $\alpha$  is 0.1, 1, and 10, respectively [Fig. 3(b)]. Gao *et al.* [19] have indicated that the stress drop in actual slow-slip phenomena is on the order of 0.1–0.01 MPa, which suggests that the value obtained in this experiment ( $\alpha = 1.03$ ) is consistent with the  $\alpha$  values in natural faults. Therefore, we set  $\alpha$  to 1.0 in the following simulations to investigate the other seismogenic parameters.

Figure 4(a) shows the relationship between the recurrence interval and stress drop based on the present model, which is obtained by varying the loading velocity from 6 to 16  $\text{cm y}^{-1}$ . These stick-slips, as mentioned earlier, encompass the entire suite of seismic events, ranging from regular earthquakes to slow-slip events, in terms of the peak velocity [Fig. 4(b)]. The magnitude of the stress drop increases linearly with recurrence time, which contrasts with the case of the frictional model

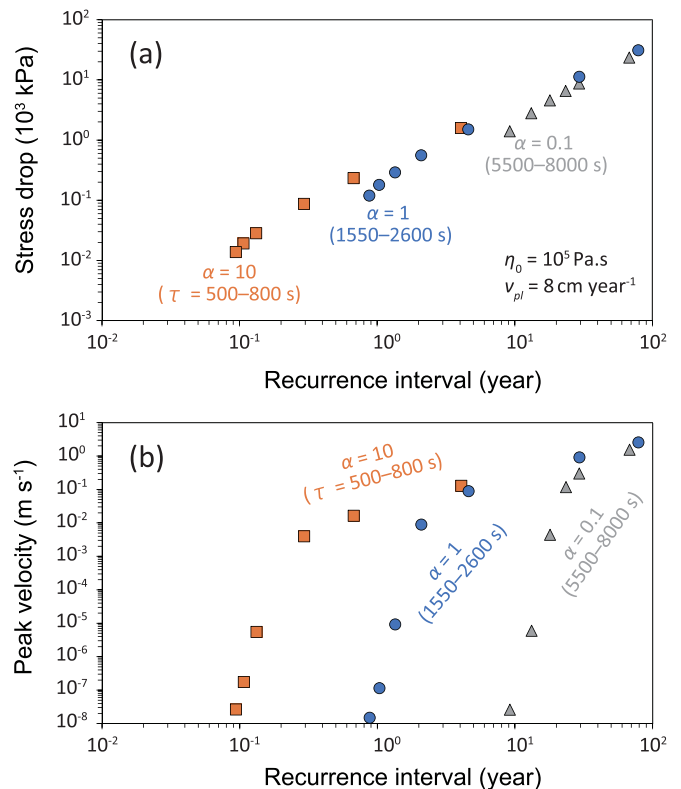


FIG. 3. (a) Stress drop vs recurrence time and (b) peak velocity vs recurrence time in periodic motion for different  $\alpha$  values ( $= 0.1, 1, 10$ ).

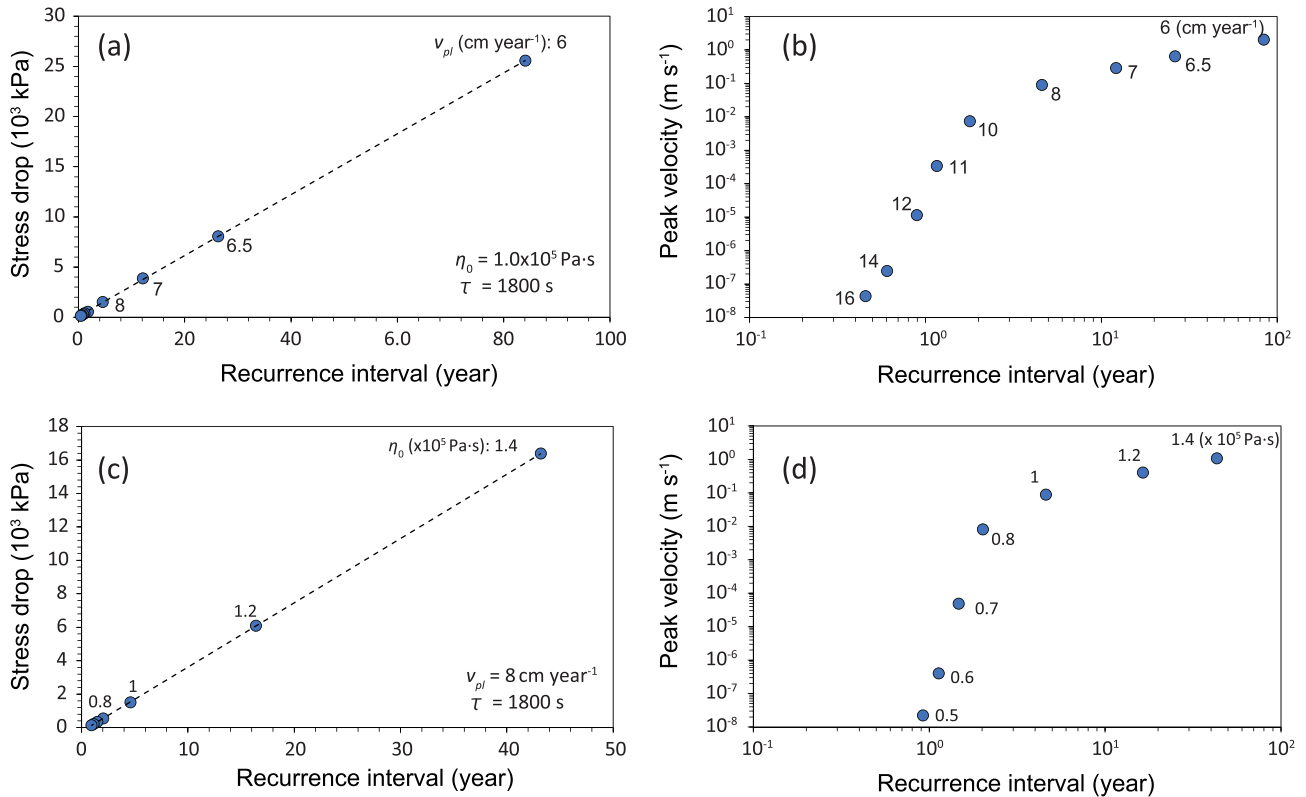


FIG. 4. (a) and (c) Stress drop vs recurrence time and (b) and (d) peak velocity vs recurrence time in periodic motion. The recurrence times in (a) and (b) are varied via the loading velocity, which ranges from 6 to 16  $\text{cm year}^{-1}$  at  $\tau = 6000 \text{ s}$ . The recurrence times in (c) and (d) are varied via the limiting viscosity, which ranges from 1.4 to  $0.5 \times 10^5 \text{ Pa}\cdot\text{s}$ .

where the magnitude of the stress drop shows a logarithmic dependence on the recurrence time of the event [20]. Figure 4 also shows the relationship between the recurrence interval and stress drop for different  $\eta_0$  [Fig. 4(c)] and the corresponding relationship between the recurrence interval and peak velocity [Fig. 4(d)]. Like the previous result, there is a linear relationship between the magnitude of the stress drop and recurrence interval.

We then examined the asymmetric features of the velocity and stress fluctuations for each system that was presented in Fig. 4(a) by differentiating the velocity and stress fluctuations to calculate their skewness and kurtosis (Fig. 5). The skewness of the velocity fluctuation is positive for the high peak velocity system (peak velocity  $> \sim 0.1 \text{ m/s}$ ) but decreases to a negative value for a lower velocity system. The skewness of the stress fluctuation also shows the similar dependence on the peak velocity to that in the case of velocity, although this skewness spans a negative range of values. These trends indicate that stick-slip motions with small peak velocities, such as slow earthquakes, are characterized by stresses and velocities that first exhibit a slow increase and then a relatively rapid decrease or deceleration [21]. This is consistent with the observation that the rise time (i.e., acceleration stage) in slow earthquakes accounts for a large proportion of the overall time of each event [19]. The kurtosis is generally inversely correlated with the skewness; when the fluctuations show symmetrical features, they likely have a long tail in the deceleration period.

#### IV. IMPLICATIONS FOR NATURAL EARTHQUAKES

The observed stick-slip behavior in our simulations can be related to the *in situ* seismic activity on the Tohoku plate-boundary fault. As mentioned earlier, precursory seismic activity occurred on the fault before the 2011 Tohoku-Oki earthquake, and the causal relationship between this antecedent activity and the mainshock has attracted much attention. In addition to  $M_w = \sim 7$  foreshocks, several precursory seismic events, including the afterslip of a foreshock, are characterized by lower rates of fault slip ( $\sim 10^{-6}$  to  $10^{-7} \text{ m s}^{-1}$ ) relative to the mainshock ( $\sim 1 \text{ m s}^{-1}$ ) [5–7]. Our simple model indicates that the fault could spontaneously slip with a range of slip velocities and recurrence intervals depending on the system parameters. More importantly, the stress state of the fault evolves with time and is highly disturbed by such seismic slip. It is likely that precursory slip events, which can occur as a spontaneous stick-slip behavior exhibited by a thixotropic fluid, disturb the microstructure of the fault zone (i.e., state variable  $\lambda$ ) and cause a significant decrease in the viscosity and shear stress immediately after the event, after which the state recovers with time, as demonstrated in Fig. 2. The focal depth of the 2011 Tohoku-Oki mainshock is deeper than the studied fault zone, which suggests that the rupture and slip propagated from depth [2]. The shallow low-viscosity (and therefore low-shear-strength) part of the megathrust fault could act as a low barrier to rupture and facilitate slip propagation, thereby serving to increase the ultimate earthquake magnitude. In other words, the magnitudes

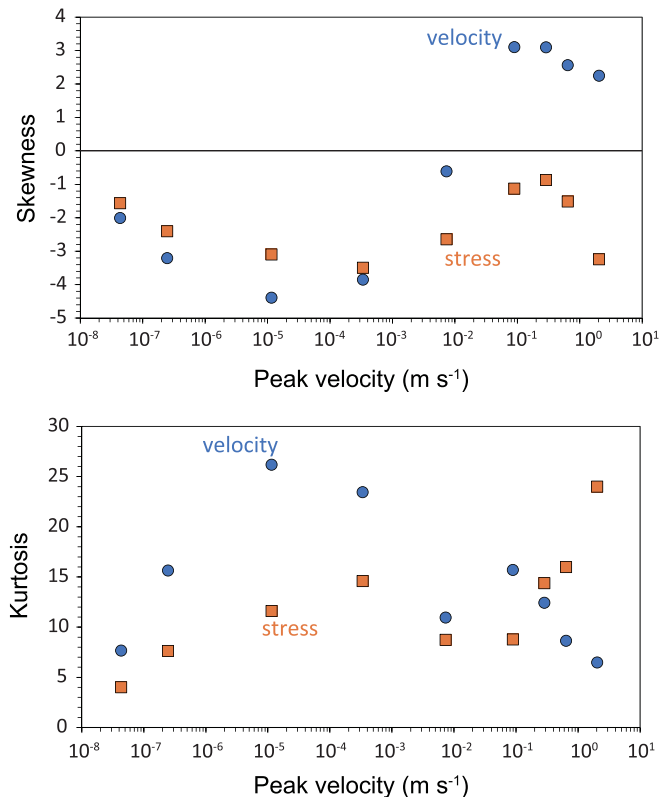


FIG. 5. Skewness (upper panel) and kurtosis (lower panel) for the stress and velocity fluctuations with respect to peak velocity. The calculation conditions are the same as in Figs. 4(a) and 4(b).

of earthquakes on this fault might be controlled by the degree to which the state variables of the fault that were perturbed by precursory earthquakes have recovered (i.e., the time interval of the propagation of rupture and slip from depth and the time constant of aging). Earthquakes with lower slip rates, such as those observed on the Tohoku-Oki fault, have been found on shallow plate-boundary faults around the world [22,23], and it is becoming clear that such faults are rich in clay (e.g., off Sumatra [24,25]). Therefore, there is a possibility that the earthquake generation model presented here can be applied to other plate-boundary earthquakes. Our model, which is deduced from the material properties of the fault, seems to reasonably reproduce some of the currently observed features of slow slips, such as the peak slip velocity, asymmetry of its variation, and magnitude of the stress drop. However, as mentioned earlier, there is a difference between the stick-slip behaviors based on the present model and those based on the conventional friction law in the relationship between the magnitude of the stress drop in each earthquake and its recurrence interval. Longer-term observations are therefore necessary to clarify the pattern of earthquake occurrence and determine which model is more appropriate for describing the dynamics of shallow faults.

#### ACKNOWLEDGMENT

This paper was supported by JSPS (Japan Society for the Promotion of Science) KAKENHI Grants No. JP18H01295 and No. JP20K14587.

- [1] C. H. Scholz, *The Mechanics of Earthquake and Faulting* (Cambridge University Press, Cambridge, 2002), p. 471.
- [2] S. Ide, A. Baltay, and G. C. Beroza, Shallow dynamic overshoot and energetic deep rupture in the 2011 Mw 9.0 Tohoku-Oki earthquake, *Science* **332**, 1426 (2011).
- [3] Y. Fujii, K. Satake, S. Sakai, M. Shinohara, and T. Kanazawa, Tsunami source of the 2011 off the Pacific coast of Tohoku earthquake, *Earth Planets Space* **63**, 815 (2011).
- [4] T. Fujiwara, S. Kodaira, T. No, Y. Kaiho, N. Takahashi, and Y. Kaneda, The 2011 Tohoku-Oki earthquake: displacement reaching the trench axis, *Science* **334**, 1240 (2011).
- [5] A. Kato, K. Obara, T. Igarashi, H. Tsuruoka, S. Nakagawa, and N. Hirata, Propagation of slow slip leading up to the 2011 Mw 9.0 Tohoku-Oki earthquake, *Science* **335**, 705 (2012).
- [6] Y. Ito, R. Hino, M. Kido, H. Fujimoto, Y. Osada, D. Inazu, Y. Ohta, T. Inuma, M. Ohzono, S. Miura, M. Mishina, K. Suzuki, T. Tsuji, and J. Ashi, Episodic slow slip events in the Japan subduction zone before the 2011 Tohoku-Oki earthquake, *Tectonophysics* **600**, 14 (2013).
- [7] M. Ikari, Y. Ito, K. Ujiie, and A. J. Kopf, Spectrum of slip behaviour in Tohoku fault zone samples at plate tectonic slip rates, *Nat. Geosci.* **8**, 870 (2015).
- [8] F. M. Chester, C. Rowe, K. Ujiie, J. Kirkpatrick, C. Regalla, F. Remitti, J. C. Moore, V. Toy, M. Wolfson-Schwehr, S. Bose *et al.*, Structure and composition of the plate-boundary slip zone for the 2011 Tohoku-Oki earthquake, *Science* **342**, 1208 (2013).
- [9] J. Kameda, M. Shimizu, K. Ujiie, T. Hirose, M. Ikari, J. Mori, K. Oohashi, and G. Kimura, Pelagic smectite as an important factor in tsunamigenic slip along the Japan Trench, *Geology* **43**, 155 (2015).
- [10] J. Kameda, M. Uno, M. Conin, K. Ujiie, Y. Hamada, and G. Kimura, Fault weakening caused by smectite swelling, *Earth Planets Space* **71**, 131 (2019).
- [11] J. Kameda and Y. Hamada, Cohesional slip on a plate subduction boundary during a large earthquake, *Geophys. Res. Lett.* **47**, e2020GL088395 (2020).
- [12] P. Coussot, Q. D. Nguyen, H. T. Huynh, and D. Bonn, Avalanche Behavior in Yield Stress Fluids, *Phys. Rev. Lett.* **88**, 175501 (2002).
- [13] P. Coussot, Q. D. Nguyen, H. T. Huynh, and D. Bonn, Viscosity bifurcation in thixotropic, yielding fluids, *J. Rheol.* **46**, 573 (2002).
- [14] A. Khalidoun, P. Moller, A. Fall, G. Wegdam, B. De Leeuw, Y. Méheust, J. O. Fossum, and D. Bonn, Quick Clay and Landslides of Clayey Soils, *Phys. Rev. Lett.* **103**, 188301 (2009).
- [15] S. R. Carrière, D. Jongmans, G. Chambon, G. Bièvre, B. Lanson, L. Bertello, M. Berti, M. Jaboyedoff, J. P. Malet, and J. E. Chambers, Rheological properties of clayey soils originating from flow-like landslides, *Landslides* **15**, 1615 (2018).
- [16] F. Pignon, A. Magnin, and J. M. Piau, Thixotropic colloidal suspensions and flow curves with minimum: identification of

- flow regimes and rheometric consequences, *J. Rheol.* **40**, 573 (1996).
- [17] G. Picard and A. Ajdari, Simple model for heterogeneous flows of yield stress fluids, *Phys. Rev. E* **66**, 051501 (2002).
- [18] P. M. Fulton, E. E. Brodsky, Y. Kano, J. Mori, F. Chester, T. Ishikawa, R. N. Harris, W. Lin, N. Eguchi, S. Toczko *et al.*, Low coseismic friction on the Tohoku-Oki fault determined from temperature measurements, *Science* **342**, 1214 (2013).
- [19] H. Gao, D. A. Schmidt, and R. J. Weldon II, Scaling relationships of source parameters for slow slip events, *Bull. Seismol. Soc. Am.* **102**, 352 (2012).
- [20] K. Im, D. Elsworth, C. Marone, and J. Leeman, The impact of frictional healing on stick-slip recurrence interval and stress drop: implications for earthquake scaling, *J. Geophys. Res. Solid Earth* **122**, 102 (2017).
- [21] J. Weiss, V. Pelisse, D. Marsan, L. Arnaud, and F. Renard, Cohesion versus friction in controlling the long-term strength of a self-healing experimental fault, *J. Geophys. Res. Solid Earth* **121**, 8523 (2016).
- [22] T. Lay, H. Kanamori, C. J. Ammon, M. Nettles, S. N. Ward, R. C. Aster, S. L. Beck, S. L. Bilek, M. R. Brudzinski, R. Butler, H. R. DeShon *et al.*, The Great Sumatra-Andaman earthquake of 26 December 2004, *Science* **308**, 1127 (2005).
- [23] K. Obara and A. Kato, Connecting slow earthquakes to huge earthquakes, *Science* **353**, 6296 (2016).
- [24] A. Hüpers, M. E. Torres, S. Owari, L. C. McNeill, B. Dugan, T. J. Henstock, K. L. Milliken, K. E. Petronotis, J. Backman, S. Bourlange, F. Chemale Jr. *et al.*, Release of mineral-bound water prior to subduction tied to shallow seismogenic slip off Sumatra, *Science* **356**, 841 (2018).
- [25] L. C. McNeill, B. Dugan, K. E. Petronotis, and the Expedition 362 Scientists, Site U1480. Sumatra Subduction Zone, in *Proceedings of the International Ocean Discovery Program (IODP) College Station, TX*, 2017), Vol. 362.